hep-ph/9603333 PITHA 96/07

March, 1996

Spin-Spin Correlations of Top Quark Pairs at Hadron Colliders

Arnd Brandenburg

Institut für Theoretische Physik, Physikzentrum

Rheinisch-Westfälische Technische Hochschule Aachen

52056 Aachen, Germany

Abstract

Top quark pairs are produced with strongly correlated spins in the partonic reactions $q\bar{q} \to t\bar{t}$ and $gg \to t\bar{t}$. A complete description of these effects in terms of the spin density matrix of the $t\bar{t}$ system in leading order QCD is given. We further discuss the prospects to observe the spin-spin correlations at $p\bar{p}$ and pp colliders by measuring suitable angular correlations among the t and $\bar{t}$ decay products.

1 Introduction

After the recent discovery of the top quark [1], the detailed study of the properties of this particle will be a major subject of experiments at the (upgraded) Tevatron and at future colliders. An intriguing feature of the top quark is that due to its heaviness it decays on average before it can form hadronic bound states. Moreover, the typical spin flip time is much larger than the lifetime of the top [2]. Thus a possible polarization of the $t\bar{t}$ system induced by the production mechanism will be transferred to its decay products. Due to the dominant parity violating decay mode $t \to Wb$ the t and $\bar{t}$ "self-analyze" their spins. The spin information may be extracted by forming angular correlations among the t and $\bar{t}$ decay products, thus allowing for a variety of tests of the standard model (SM) and extensions thereof (see, e.g. [3]- [23]).

While at hadron colliders the *longitudinal* polarization of top quarks is practically zero due to parity invariance of QCD, a nonzero polarization *transverse* to the production plane is induced by absorptive parts at the one-loop level. The prospects to observe this order α_s effect at the Tevatron and the Large Hadron Collider (LHC) have been studied in detail in [21] (see also [7],[11]). Apart from this single quark polarization, the t and $\bar{t}$ are produced with *strongly correlated spins* in $q\bar{q} \to t\bar{t}$ and $gg \to t\bar{t}$, which are the dominant partonic production processes at the Tevatron and the LHC, respectively. In fact, these spin-spin correlations are of order one at the level of the partonic reactions. It is the aim of this letter to discuss the prospects to unravel these effects. An experimental verification of the feasibility to extract spin information on top quarks would clearly be important for any further proposals to study quantities related to the top spin.

In the next section we will give a general description of the $t\bar{t}$ spin state in terms of a spin density matrix. QCD induced spin-spin correlations may be described in general by four "structure functions". The leading order results for these functions are given. Observables built from the spin operators of t and $\bar{t}$ allow to discuss the magnitude of the correlations at parton level. In Section 3 we will construct observables which are directly measurable (on an event by event basis) in $p\bar{p}, pp \to t\bar{t}X$ with subsequent $t\bar{t}$ decays.

2 The spin density matrices for $q\bar{q} \to t\bar{t}$ and $gg \to t\bar{t}$

Although the spin of an unstable particle produced in high-energy reactions is no directly observable quantity, it is very useful to introduce the concept of a *spin density matrix* for the $t\bar{t}$ system. Using the narrow width approximation for the top quark, we may view the reactions considered here as the production and subsequent decay of on-shell top quark pairs. The spin information may then be extracted on a statistical basis from the decay products of the t and $\bar{t}$.

We first discuss the reaction $q(p_1) + \bar{q}(p_2) \to t(k_1) + \bar{t}(k_2)$, where the momenta refer to the partonic c.m. system, $\boldsymbol{p}_1 + \boldsymbol{p}_2 = 0$. The complete spin information is encoded in the (unnormalized) spin density matrix R^q,

$$R^q_{\alpha_1\alpha_2,\beta_1\beta_2}(\boldsymbol{p},\boldsymbol{k}) = \frac{1}{4}\frac{1}{N_C^2}\sum_{\text{colors},q\bar{q}\text{ spins}} \langle t(k_1,\alpha_1)\bar{t}(k_2,\beta_1)|\mathcal{T}|q(p_1),\bar{q}(p_2)\rangle^* \\ \langle t(k_1,\alpha_2)\bar{t}(k_2,\beta_2)|\mathcal{T}|q(p_1),\bar{q}(p_2)\rangle. \tag{1}$$

Here, $\alpha,\ \beta$ are spin indices, N_C denotes the number of colors, $\boldsymbol{p} = \boldsymbol{p}_1,\ \boldsymbol{k} = \boldsymbol{k}_1$ and the sum runs over the colors of all quarks and over the spins of q and $\bar{q}$. The factor $1/4 \cdot 1/N_C^2$ takes care of the averaging over spins and colors in the initial state. The matrix structure of R^q in the spin spaces of t and $\bar{t}$ is

$$R^q = A^q 1\!\!1 \otimes 1\!\!1 + \boldsymbol{B}^q_t \cdot \boldsymbol{\sigma} \otimes 1\!\!1 + \boldsymbol{B}^q_{\bar{t}} \cdot 1\!\!1 \otimes \boldsymbol{\sigma} + C^q_{ij}\sigma^i \otimes \sigma^j, \tag{2}$$

where σ^i are the Pauli matrices and the first (second) factor in the tensor products refers to the t ($\bar{t}$) spin space. (The spin operators of t and $\bar{t}$ are simply given by $\boldsymbol{\sigma}/2 \otimes 1\!\!1$ and $1\!\!1 \otimes \boldsymbol{\sigma}/2$.) For a detailed discussion of R^q and its symmetry properties, see [16]. We will now specialize on reactions mediated by strong interactions. Imposing P and CP invariance on R_q and using rotational invariance, we are left with the following structures:

$$\begin{aligned} A^q &= \frac{8\pi\hat{s}}{\beta}\frac{d\hat{\sigma}^q}{dz}, \\ \boldsymbol{B}^q_t &= \boldsymbol{B}^q_{\bar{t}} = b^q_3(\hat{s},z)\frac{\boldsymbol{p}\times\boldsymbol{k}}{|\boldsymbol{p}\times\boldsymbol{k}|} && (3) \\ C^q_{ij} &= c^q_0(\hat{s},z)\delta_{ij} + c^q_4(\hat{s},z)\hat{p}_i\hat{p}_j + c^q_5(\hat{s},z)\hat{k}_i\hat{k}_j + c^q_6(\hat{s},z)(\hat{p}_i\hat{k}_j + \hat{k}_i\hat{p}_j). && (4) \end{aligned}$$

Here, $\beta = \sqrt{1 - 4m_t^2/\hat{s}}$ is the velocity of the top quark in the partonic c.m. system, $\hat{\boldsymbol{p}} = \boldsymbol{p}/|\boldsymbol{p}|$, $\hat{\boldsymbol{k}} = \boldsymbol{k}/|\boldsymbol{k}|$, $z = \hat{\boldsymbol{p}} \cdot \hat{\boldsymbol{k}}$ is the scattering angle and $\hat{s} = (p_1 + p_2)^2$ is the partonic c.m. energy squared. (The notation, in particular the numbering, is adopted from [16].) For $gg \to t\bar{t}$ we have an analogous decomposition with $1/N_C^2 \to 1/(N_C^2 - 1)^2$ in (1). The functions b_3^i, $i = q, g$ derive from absorptive parts in the scattering amplitude [21]. Here we are interested in the spin-spin correlation functions c_0^i, c_4^i, c_5^i and c_6^i. They are already induced at Born level. The leading order results can be found in [16]. We give them here in a compact form for completeness.

$\underline{q\bar{q} \to t\bar{t}}$

Define $\kappa_q = \pi^2 \alpha_s^2 \dfrac{N_C^2 - 1}{N_C^2}$. Then

$$
\begin{aligned}
A^q &= \kappa_q (2 + (z^2 - 1)\beta^2), \\
c_0^q &= \kappa_q (z^2 - 1)\beta^2, \\
c_4^q &= 2\kappa_q, \\
c_5^q &= 2\kappa_q \beta^2 \left(1 + \frac{z^2\beta^2}{(1 + \sqrt{1 - \beta^2})^2}\right), \\
c_6^q &= -2\kappa_q \frac{z\beta^2}{1 + \sqrt{1 - \beta^2}}.
\end{aligned} \tag{5}
$$

$\underline{gg \to t\bar{t}}$

Using the abbreviation $\kappa_g = \dfrac{\pi^2 \alpha_s^2}{(1 - z^2\beta^2)^2} \dfrac{N_C^2 - 2 + N_C^2 z^2 \beta^2}{N_C(N_C^2 - 1)}$ we have

$$
\begin{aligned}
A^g &= 2\kappa_g \left[1 + 2\beta^2(1 - z^2)(1 - \beta^2) - \beta^4 z^4\right], \\
c_0^g &= -2\kappa_g \left[(1 - \beta^2)^2 + \beta^4(1 - z^2)^2)\right], \\
c_4^g &= 4\kappa_g (1 - z^2)\beta^2, \\
c_5^g &= -4\kappa_g \beta^2 \left(1 - 2\beta^2 + z^2\beta^2 - \frac{z^2\beta^4(1 - z^2)}{(1 + \sqrt{1 - \beta^2})^2}\right), \\
c_6^g &= -4\kappa_g \frac{z(1 - z^2)\beta^4}{1 + \sqrt{1 - \beta^2}}.
\end{aligned} \tag{6}
$$

Due to Bose symmetry, $R^g(\boldsymbol{p}, \boldsymbol{k}) = R^g(-\boldsymbol{p}, \boldsymbol{k})$, which means that $c_{0,4,5}^g$ are even functions of z whereas c_6 is odd in z. In leading order, the structure functions for $q\bar{q} \to t\bar{t}$

have the same symmetry properties, because the reaction proceeds through a single virtual intermediate gluon, implying that also R^q is invariant under $\boldsymbol{p} \to -\boldsymbol{p}$.

We may now construct a list of "observables" built from the spin operators of t and $\bar{t}$:

$$\begin{aligned}
\hat{\mathcal{O}}^i_1 &= \boldsymbol{\sigma} \otimes \boldsymbol{\sigma}, \\
\hat{\mathcal{O}}^i_2 &= \hat{\boldsymbol{p}} \cdot \boldsymbol{\sigma} \otimes \hat{\boldsymbol{p}} \cdot \boldsymbol{\sigma}, \\
\hat{\mathcal{O}}^i_3 &= \hat{\boldsymbol{k}} \cdot \boldsymbol{\sigma} \otimes \hat{\boldsymbol{k}} \cdot \boldsymbol{\sigma}, \\
\hat{\mathcal{O}}^i_4 &= (\hat{\boldsymbol{p}} \cdot \boldsymbol{\sigma} \otimes \hat{\boldsymbol{k}} \cdot \boldsymbol{\sigma} + \hat{\boldsymbol{p}} \cdot \boldsymbol{\sigma} \otimes \hat{\boldsymbol{k}} \cdot \boldsymbol{\sigma})/2 \qquad (i = q, g).
\end{aligned} \tag{7}$$

At the level of $t\bar{t}$ production from partons the expectation values of these quantities for fixed $\hat{s}$ and z are defined as

$$\langle \hat{\mathcal{O}}^i_{1,2,3,4} \rangle = \frac{\mathrm{tr}(R^i \hat{\mathcal{O}}^i_{1,2,3,4})}{\mathrm{tr}(R^i)}, \tag{8}$$

where the trace is over the spin spaces of t and $\bar{t}$. They are given by linear combinations of the functions $c^i_0(\hat{s}, z), \ldots, c^i_6(\hat{s}, z)$, divided by the unpolarized differential cross section $A^i(\hat{s}, z)$. In particular, we find

$$\langle \hat{\mathcal{O}}^q_1 \rangle = 1, \tag{9}$$

which can be easily understood from the fact that the $t\bar{t}$ pair is produced from a single spin one boson in $q\bar{q}$ collisions at Born level. At threshold, one can show that the quantum numbers of the top quark pair are given by ${}^3S_1$ for $q\bar{q} \to t\bar{t}$ and ${}^1S_0$ for $gg \to t\bar{t}$ [9],[15]. In particular,

$$\lim_{\beta \to 0} \langle \hat{\mathcal{O}}^g_1 \rangle = -3, \tag{10}$$

which can be verified using (6). As a further example we plot in fig.1 the rapidity distribution of $\langle \hat{\mathcal{O}}^q_3 \rangle$, defined by

$$\frac{\int_{-1}^{1} dz \ \mathrm{tr}(R^q \hat{\mathcal{O}}^q_3) \delta(\hat{r}_t - \hat{r}'_t)}{\int_{-1}^{1} dz \ \mathrm{tr}(R^q)} \tag{11}$$

with

$$\hat{r}_t = \frac{1}{2} \ln \left(\frac{1 + \beta z}{1 - \beta z} \right) \tag{12}$$

at a value $\beta = 0.5$. We choose the rapidity of the top quark in the partonic c.m. system as variable here instead of the scattering angle for later comparison with observables for $pp, p\bar{p} \to t\bar{t}X \to \dots$, for which rapidity is a convenient variable.

The expectation value $\langle \hat{\mathcal{O}}_3^i \rangle$ corresponds to a helicity correlation studied by Stelzer and Willenbrock [23] and also by Mahlon and Parke [22], namely

$$\langle \hat{\mathcal{O}}_3^i \rangle = -\frac{d\hat{\sigma}^i(t_R\bar{t}_R + t_L\bar{t}_L)/dz - d\hat{\sigma}^i(t_R\bar{t}_L + t_L\bar{t}_R)/dz}{d\hat{\sigma}^i(t_R\bar{t}_R + t_L\bar{t}_L)/dz + d\hat{\sigma}^i(t_R\bar{t}_L + t_L\bar{t}_R)/dz}. \tag{13}$$

Here, the indices L and R correspond to left- and right handed particles, respectively, and $d\hat{\sigma}^i$ denotes the partonic cross section, $i = q, g$. We find agreement with the values given in [23] for this correlation integrated over the scattering angle and folded with the parton distribution functions both for Tevatron and LHC energies (+40% and −31%, respectively). Rather than to specialize on finding ways to trace this correlation of helicities, we will in the following try to extract as much information on the spin density matrix as possible, i.e. construct angular correlations among the $t\bar{t}$ decay products in close correspondence to all four "partonic" observables defined in (7).

3 Angular correlations for semileptonic $t\bar{t}$ decays

The spin-spin correlations discussed in the previous section must be traced in the decay products of the t and $\bar{t}$. The spin information in the production density matrices R^i is transferred to the decay products through the parity violating decays of the top quarks. For semileptonic decays $t \to \ell^+\nu_{\ell^+}b$, the normalized *decay spin density matrix* ρ of the top quark in leading order (and using the narrow width approximation for the W boson) reads (see, e.g., [12])

$$\rho(t \to \ell^+\nu_{\ell^+}b) = \frac{6x_{\ell^+}(1-x_{\ell^+})}{(1+2\omega)(1-\omega)^2}\left[1\!\!1 + \hat{\mathbf{q}}^*_{\ell^+}\cdot\boldsymbol{\sigma}\right]\frac{dx_{\ell^+}d\Omega_{\ell^+}}{4\pi}, \tag{14}$$

where $\omega = m_W^2/m_t^2$, $x_{\ell^+} = 2E^*_{\ell^+}/m_t \in [\omega, 1]$ is the scaled energy of the lepton, and $\hat{\mathbf{q}}^*_{\ell^+}$ is the direction of the lepton. The asterisk refers to the rest system of the decaying quark. For hadronic decays, $t \to W^+b \to bq\bar{q}'$, we have, if we use the tagged b quark as spin

analyzer,

$$\rho(t \to W^+ b \to b q \bar{q}') = \left[1\!\!1 + \frac{2\omega - 1}{2\omega + 1} \hat{\mathbf{q}}_b^* \cdot \boldsymbol{\sigma} \right] \frac{d\Omega_b}{4\pi}. \tag{15}$$

The corresponding decay spin density matrices $\bar{\rho}$ for the top antiquark are derived from the above ones by the replacements $x_{\ell^+} \to x_{\ell^-}$, $\hat{\mathbf{q}}_{\ell^+}^* \to -\hat{\mathbf{q}}_{\ell^-}^*$ and $d\Omega_{\ell^+} \to d\Omega_{\ell^-}$ in (14) and by $\hat{\mathbf{q}}_b^* \to -\hat{\mathbf{q}}_{\bar{b}}^*$, $d\Omega_b \to d\Omega_{\bar{b}}$ in (15). We may also use the W boson as spin analyzer instead of the b quark. We get the corresponding decay density matrix from (15) by $\hat{\boldsymbol{q}}_b^* \to -\hat{\boldsymbol{q}}_{W^+}^*$, $d\Omega_b \to d\Omega_{W^+}$. In particular, the W boson has the same spin analyzer quality as the b quark. The expectation value of any observable constructed from the momenta of the final state particles will involve a trace over the spin spaces of t and $\bar{t}$ of the form $\mathrm{tr}\left[R^i \rho(t \to X) \otimes \bar{\rho}(\bar{t} \to \bar{X}')\right]$. Thus the spin information of the production density matrix R^i is recovered in the decay products in a statistical sense.

We will concentrate on decay channels where either the t or the $\bar{t}$ decays leptonically and the other quark decays hadronically, i.e. on the decay modes

$$\begin{aligned} t &\to W^+ b \to b q \bar{q}', \\ \bar{t} &\to \ell^- \bar{\nu}_{\ell^-} \bar{b} \end{aligned} \tag{16}$$

and the charge conjugated ones. These decay modes turn out to be especially suited to construct observables which are sensitive to spin-spin correlations: The charged lepton is the most efficient spin analyzer (cf.(14)), while in the same event the momentum of the top quark (or antiquark) may be reconstructed from its hadronic decay products. For nonleptonic decays, since charm tagging is difficult, we will use the bottom quark as spin analyzer. (Alternatively, we may use the W boson.) This leads to a suppression factor $(1 - 2\omega)/(1 + 2\omega) \approx 0.43$ in all quantities we will discuss. One may also consider double leptonic decays where this suppression factor is absent. However, apart from forming only $\sim 1/9$ of all $t\bar{t}$ decays, these events do not allow for a reconstruction of the t and/or $\bar{t}$ rest system on an event-by-event basis due to the unseen neutrinos. Any correlation constructed from the laboratory momenta of the two charged leptons suffers from a large "background" from the unpolarized cross section, i.e. A^i of eqs. (5, 6). In contrast, the quantities we will use get contributions from spin-spin correlations only.

In close correspondence to the observables (7) we define, for the decay modes (16):

$$\begin{aligned}
\mathcal{O}_1 &= \hat{\boldsymbol{q}}_b^* \cdot \hat{\boldsymbol{q}}_{\ell^-}, \\
\mathcal{O}_2 &= (\hat{\boldsymbol{q}}_b^* \cdot \hat{\boldsymbol{p}}_p)(\hat{\boldsymbol{q}}_{\ell^-} \cdot \hat{\boldsymbol{p}}_p), \\
\mathcal{O}_3 &= (\hat{\boldsymbol{q}}_b^* \cdot \hat{\boldsymbol{k}}_t)(\hat{\boldsymbol{q}}_{\ell^-} \cdot \hat{\boldsymbol{k}}_t), \\
\mathcal{O}_4 &= \left[(\hat{\boldsymbol{q}}_b^* \cdot \hat{\boldsymbol{p}}_p)(\hat{\boldsymbol{q}}_{\ell^-} \cdot \hat{\boldsymbol{k}}_t) + (\hat{\boldsymbol{q}}_b^* \cdot \hat{\boldsymbol{k}}_t)(\hat{\boldsymbol{q}}_{\ell^-} \cdot \hat{\boldsymbol{p}}_p)\right]/2.
\end{aligned} \tag{17}$$

Here, quantities without an asterisk are defined in the laboratory frame, carets denote unit vectors and $\hat{\boldsymbol{p}}_p$ is the beam direction. The top quark momentum $\boldsymbol{k}_t$ has to be reconstructed from its hadronic decay products for a measurement of $\mathcal{O}_1, \ldots \mathcal{O}_4$. The momentum of the b quark was boosted into the top quark rest system*. Analogous observables $\bar{\mathcal{O}}_{1,2,3,4}$ may be defined for the charge conjugated decay modes. The observable $\mathcal{O}_4$ gives zero if integrated over a symmetric rapidity interval in our leading order calculation because, as discussed above, $R^{g,q}(\boldsymbol{p}, \boldsymbol{k}) = R^{g,q}(-\boldsymbol{p}, \boldsymbol{k})$. We therefore also define

$$\mathcal{O}_5 = \mathrm{sign}(r_t)\mathcal{O}_4, \tag{18}$$

with

$$r_t = \frac{1}{2}\ln\left(\frac{E_t + \hat{\boldsymbol{p}}_p \cdot \boldsymbol{k}_t}{E_t - \hat{\boldsymbol{p}}_p \cdot \boldsymbol{k}_t}\right). \tag{19}$$

We evaluated the correlations $\langle \mathcal{O}_j \rangle$ $(j = 1, 2, 3, 5)$ for $p\bar{p}$ collisions between 1.6 and 4 TeV and for pp collisions between 8 and 16 TeV with $m_t = 180$ GeV. We found only a weak dependence on the choice of the parton distribution functions. In the results below, we used the parametrization [24] with $Q^2 = 4m_t^2$. We applied cuts on the top quark transverse momentum $|\boldsymbol{k}_t^T|$ and rapidity: For the lower energies, we used $|\boldsymbol{k}_t^T| > 15$ GeV, $|r_t| < 2$, for the higher energies, the cuts $|\boldsymbol{k}_t^T| > 20$ GeV, $|r_t| < 3$ were imposed.

*A note of caution: The top quark rest frame defined in equation (14) and (15) is different from the one defined in (17); the former is defined through a rotation-free boost from the partonic c.m. system (where the matrix R^i is defined), while the latter is related to the hadronic c.m. system through a pure boost. Thus they differ by a Wigner rotation which has to be taken into account in the theoretical calculation of the expectation values of the observables (17) .

We will first discuss the case of $p\bar{p}$ collisions. The results are shown in fig. 2. The correlations are largest for small c.m. energies; there the correlation $\langle\mathcal{O}_2\rangle$ reaches a value $\sim 3.5\%$. The analogous correlations for the charge conjugated decays of the top quark pair have exactly the same values due to CP invariance. It might seem surprising that the effects are quite small remembering that we had spin-spin correlations of order one at the level of $t\bar{t}$ production from partons, cf. (9). The suppression comes about as follows: As mentioned before, we lose a factor of 0.43 by using the b quark (or W boson) as spin analyzer. Moreover, integrating over the directions of the b quark and of the charged lepton generates roughly a factor of 1/9; thus the magnitude of an angular correlation built from these directions is $\sim 5\%$. This is the price we have to pay for using observables which can be measured on an event-by-event basis and are strictly zero in the absence of spin-spin correlations. We will now consider signal-to-noise ratios in order to estimate the statistical significance of the correlations. The statistical fluctuations of our observables are given by $\Delta\mathcal{O}_j = \sqrt{\langle\mathcal{O}_j^2\rangle - \langle\mathcal{O}_j\rangle^2}$. We find $\Delta\mathcal{O}_1 \approx 0.58$ for all energies (since $\langle\mathcal{O}_1^2\rangle = 1/3$) and, at $\sqrt{s} = 1.8$ TeV, $\Delta\mathcal{O}_2 \approx 0.36$, $\Delta\mathcal{O}_3 \approx 0.36$, $\Delta\mathcal{O}_5 \approx 0.25$. Measuring the analogous correlations for the charge conjugated decays increases the statistical sensitivity. For example, if $N_{b\ell^-}$ denotes the number of b-tagged, reconstructed events of type (16), and we have the same number of events in the charge conjugated channel, we get a statistical significance S_2 for the combined correlations $\langle\mathcal{O}_2\rangle$ and $\langle\bar{\mathcal{O}}_2\rangle$ of

$$S_2 \equiv \frac{|\langle\mathcal{O}_2\rangle + \langle\bar{\mathcal{O}}_2\rangle|}{\sqrt{2}\Delta\mathcal{O}_2}\sqrt{N_{b\ell^-}} \approx 0.14\sqrt{N_{b\ell^-}} \tag{20}$$

at $\sqrt{s} = 1.8$ TeV. In order to establish the spin-spin correlation at the 3σ level, we would therefore need $N_{b\ell^-} \approx 500$, which is in reach of the upgraded Tevatron. For the other three correlations shown in fig. 2, we find the following statistical sensitivities at $\sqrt{s} = 1.8$ TeV, again combining the decay modes (16) with the charge conjugated ones: $S_1 \approx 0.076\sqrt{N_{b\ell^-}}$, $S_3 \approx 0.077\sqrt{N_{b\ell^-}}$, $S_5 \approx 0.13\sqrt{N_{b\ell^-}}$.

In fig. 3 we show the rapidity distributions $\langle\mathcal{O}_1\delta(r_t - r_t')\rangle, \ldots, \langle\mathcal{O}_4\delta(r_t - r_t')\rangle$ for $\sqrt{s} = 1.8$ TeV. Note the similarity of $\langle\mathcal{O}_3\delta(r_t - r_t')\rangle$ (dotted line in fig. 3) and the corresponding rapidity distribution (11) of the correlation $\langle\mathcal{O}_3^q\rangle$ in fig. 1. This similarity

in form is to be expected, since the partonic process $q\bar{q} \to t\bar{t}$ dominates at Tevatron energies. It also holds for the other correlations and their counterparts in $q\bar{q} \to t\bar{t}$.

We now turn to pp collisions. All four correlations in this case only depend weakly on the pp c.m. energy. Between $\sqrt{s} = 8 - 16$ TeV they take the values $\langle \mathcal{O}_1 \rangle \approx (-2.37) - (-2.23)\%$, $\langle \mathcal{O}_2 \rangle \approx (-0.13) - (-0.24)\%$, $\langle \mathcal{O}_3 \rangle \approx (-0.72) - (-0.68)\%$, and $\langle \mathcal{O}_5 \rangle \approx (-0.25) - (-0.33)\%$. Note especially the smallness of $\langle \mathcal{O}_2 \rangle$, which in the case of $p\bar{p}$ collisons around $\sqrt{s} \sim 2$ TeV was the most sensitive correlation. We again get the same numbers for the charge conjugated decay modes. At $\sqrt{s} = 14$ TeV, we also determined the statistical fluctuations of the observables; as mentioned before, $\Delta\mathcal{O}_1 \approx 0.58$, and the other values are $\Delta\mathcal{O}_2 \approx 0.42$, $\Delta\mathcal{O}_3 \approx 0.38$, $\Delta\mathcal{O}_5 \approx 0.29$. Assuming again an equal number of events in the decay channel (16) and the charge conjugated one, we get by combining both correlations the following statistical sensitivities at the LHC: $\mathcal{S}_1 \approx 0.055\sqrt{N_{b\ell^-}}$, $\mathcal{S}_2 \approx 0.007\sqrt{N_{b\ell^-}}$, $\mathcal{S}_3 \approx 0.025\sqrt{N_{b\ell^-}}$, and $\mathcal{S}_5 \approx 0.016\sqrt{N_{b\ell^-}}$. Here it is useful to consider also

$$\mathcal{O}_6 \equiv (\hat{\boldsymbol{p}}_p \times \hat{\boldsymbol{q}}_b^*) \cdot (\hat{\boldsymbol{p}}_p \times \hat{\boldsymbol{q}}_{\ell^-}) = \mathcal{O}_1 - \mathcal{O}_2. \tag{21}$$

Since $\langle \mathcal{O}_6^2 \rangle = \langle \mathcal{O}_1^2 \rangle - \langle \mathcal{O}_2^2 \rangle$, we find for the combined correlations $\langle \mathcal{O}_6 \rangle$ and $\langle \bar{\mathcal{O}}_6 \rangle$ a statistical sensitivity of $\mathcal{S}_6 \approx 0.073\sqrt{N_{b\ell^-}}$ at the LHC. Note that in $\mathcal{O}_6$ effects of the boost from the partonic c.m. system to the laboratory frame drop out.

The effects are smaller at the LHC than at the Tevatron, but we have many more events. For example, assuming $N_{b\ell^-} = 10^4 = N_{\bar{b}\ell^+}$, we can establish the spin-spin correlations to 7.3σ by measuring $\mathcal{O}_6$ and $\bar{\mathcal{O}}_6$. In fig. 4 we show the rapidity distributions of the correlations at $\sqrt{s} = 14$ TeV. Due to the dominance of gluon fusion at LHC energies, the shapes of the curves are similar to the corresponding rapidity distributions of the correlations at parton level $\langle \mathcal{O}^g_{1,2,3,4} \rangle$ defined in (7).

4 Conclusions

We have shown that the sizable spin-spin correlations induced at leading order QCD in $q\bar{q} \to t\bar{t}$ and $gg \to t\bar{t}$ may be measured both at the Tevatron and the LHC. For such

measurements, angular correlations among the decay products in "semihadronic" $t\bar{t}$ decays are especially suited. The correlations we propose get nonzero contributions only from $t\bar{t}$ spin-spin correlations — which are predicted by perturbative QCD. All calculations were performed at leading order and using the narrow width approximation for the top quark. At present, NLO corrections are only known for the functions $A^{q,g}$ in (5), (6) which determine the production rate of $t\bar{t}$ pairs [25]. For a more refined theoretical study of the spin-spin correlations, we would need the complete spin density matrix in NLO as well as an estimate of the effects of non-factorizable contributions [26]. In summary, the experimental study of spin-spin correlations of top quark pairs seems very interesting and feasible.

Acknowledgements

I would like to thank W. Bernreuther, L. M. Sehgal and P. Uwer for helpful discussions, and the CERN TH Division, where part of this work was done, for hospitality and partial support.

References

[1] F. Abe et al., CDF Collaboration, Phys. Rev. Lett. **74** (1995) 2626; S. Abachi et al., D0 Collaboration, Phys. Rev. Lett. **74** (1995) 2632.

[2] I. Bigi et al., Phys. Lett. **B 181** (1986) 157.

[3] G. L. Kane, J. Pumplin, and W. Repko, Phys. Rev. Lett. **41** (1978) 1689.

[4] J. H. Kühn, A. Reiter, and P. Zerwas, Nucl. Phys. **B 272** (1986) 560.

[5] M. Anselmino, P. Kroll, and B. Pire, Phys. Lett. **B 167** (1986) 113.

[6] V. Barger, J. Ohnemus, and R.J.N. Phillips, Int. J. Mod. Phys. **A 4** (1989) 617.

[7] W. G. D. Dharmaratna and G. R. Goldstein, Phys. Rev. **D 41** (1990) 1731; Phys. Rev. **D 53** (1996) 1073.

[8] A. Czarnecki, M. Jezabek, and J. H. Kühn, Nucl. Phys. **B 351** (1991) 70.

[9] Y. Hara, Prog. Theor. Phys. **86** (1991) 779.

[10] R. H. Dalitz and G. R. Goldstein, Phys. Rev. **D 45** (1992) 1531.

[11] G. L. Kane, G. A. Ladinsky, and C.-P. Yuan, Phys. Rev. **D 45** (1992) 124.

[12] W. Bernreuther, O. Nachtmann, P. Overmann, and T. Schröder, Nucl. Phys. **B 388** (1992) 53; **B 406** (1993) 516 (E); A. Brandenburg and J. P. Ma, Phys. Lett. **B 298** (1993) 211.

[13] W. Bernreuther, J. P. Ma, and T. Schröder, Phys. Lett. **B 297** (1992) 318.

[14] D. Atwood and A. Soni, Phys. Rev. **D 45** (1992) 2405.

[15] T. Arens and L. M. Sehgal, Phys. Lett. **B 302** (1993) 501; Nucl. Phys. **B 393** (1993) 46.

[16] W. Bernreuther and A. Brandenburg, Phys. Lett. **B 314** (1993) 104; Phys. Rev. **D 49** (1994) 4481.

[17] W. Bernreuther, J. P. Ma, and B. H. J. McKellar, Phys. Rev. **D 51** (1995) 2475.

[18] J. G. Körner, A. Pilaftsis, and M. M. Tung, Z. Phys. **C 63** (1994) 575; S. Groote, J. G. Körner, and M. M. Tung, Mainz preprint MZ-TH/95-09 (1995).

[19] R. Harlander, M. Jezabek, J. H. Kühn, and T. Teubner, Phys. Lett. **B 346** (1995) 137.

[20] P. Haberl, O. Nachtmann, and A. Wilch, Heidelberg preprint HD-THEP-95-25 (1995).

[21] W. Bernreuther, A. Brandenburg, and P. Uwer, Phys. Lett. **B 368** (1996) 153.

[22] G. Mahlon and S. Parke, Fermilab-Pub-95/362-T, UM-TH-95-26, hep-ph/9512264 (1995).

[23] T. Stelzer and S. Willenbrock, ILL-(TH)-95-33, hep-ph/9512292 (1995).

[24] J. F. Owens, Phys. Lett. **B 266** (1991) 126.

[25] P. Nason, S. Dawson, and R.K. Ellis, Nucl. Phys. **B 303** (1988) 607; *ibid.* **327** (1989) 49; W. Beenakker et al., Phys. Rev. **D 40** (1989) 54; W. Beenakker et al., Nucl. Phys. **B 351** (1991) 507.

[26] K. Melnikov and O. Yakovlev, Phys. Lett. **B 324** (1994) 2171; V. S. Fadin, V. A. Khoze, and A. D. Martin, Phys. Rev. **D 49** (1994) 2247.

Figure Captions

Fig. 1 Rapidity distribution (11) of $\langle \hat{\mathcal{O}}_3^q \rangle$ at $\beta = 0.5$.

Fig. 2 Correlations $\langle \mathcal{O}_1 \rangle$ (full line), $\langle \mathcal{O}_2 \rangle$ (dashed line), $\langle \mathcal{O}_3 \rangle$ (dotted line), and $\langle \mathcal{O}_5 \rangle$ (dash-dotted line) as a function of the c.m. energy for $p\bar{p}$ collisions.

Fig. 3 Rapidity distributions $\langle \mathcal{O}_1 \delta(r_t - r_t') \rangle$ (full line), $\langle \mathcal{O}_2 \delta(r_t - r_t') \rangle$ (dashed line), $\langle \mathcal{O}_3 \delta(r_t - r_t') \rangle$ (dotted line), and $\langle \mathcal{O}_4 \delta(r_t - r_t') \rangle$ (dash-dotted line), at $\sqrt{s} = 1.8$ TeV for $p\bar{p}$ collisions.

Fig. 4 Same as Fig. 3, but for pp collisions at $\sqrt{s} = 14$ TeV.

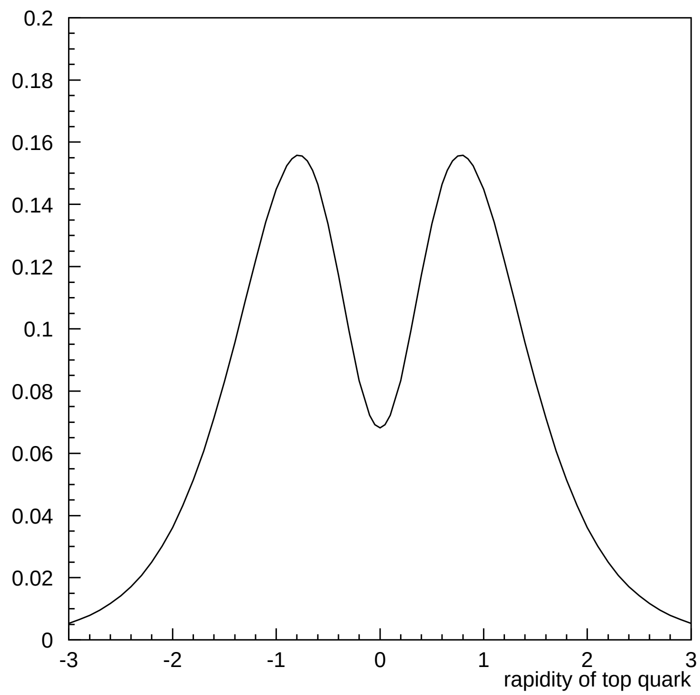
0.2
0.18
0.16
0.14
0.12
0.1
0.08
0.06
0.04
0.02
0
-3
-2
-1
0
1
2
3
rapidity of top quark

Fig. 1

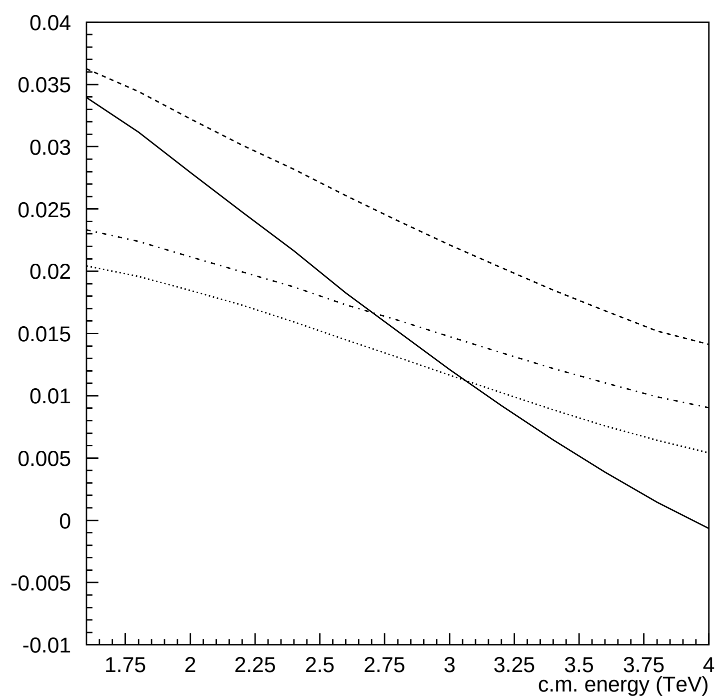
0.04
0.035
0.03
0.025
0.02
0.015
0.01
0.005
0
-0.005
-0.01
1.75
2
2.25
2.5
2.75
3
3.25
3.5
3.75
4
c.m. energy (TeV)

Fig. 2

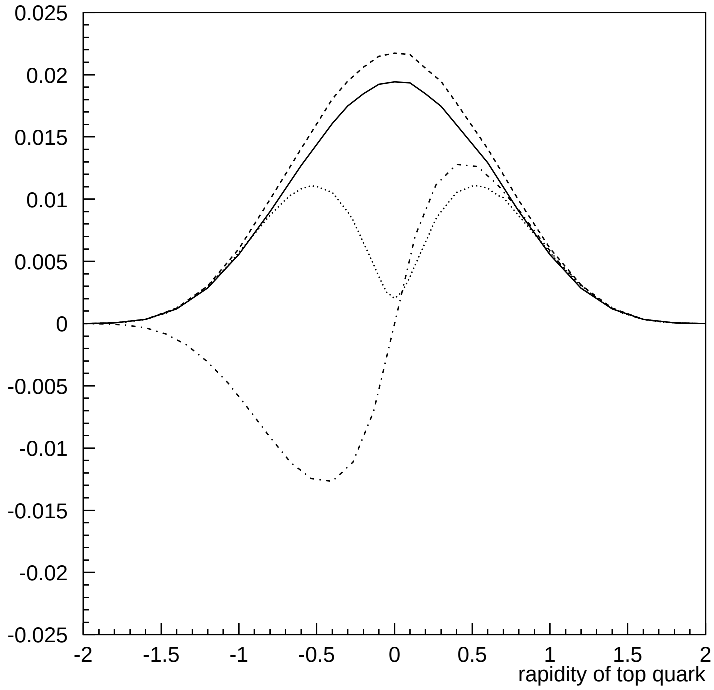
0.025
0.02
0.015
0.01
0.005
0
-0.005
-0.01
-0.015
-0.02
-0.025
-2
-1.5
-1
-0.5
0
0.5
1
1.5
2
rapidity of top quark

Fig. 3

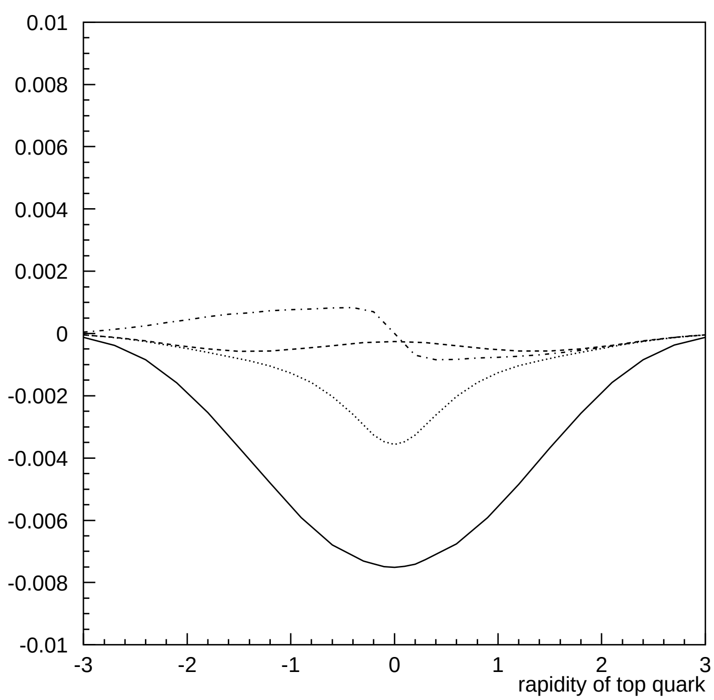
0.01
0.008
0.006
0.004
0.002
0
-0.002
-0.004
-0.006
-0.008
-0.01
-3
-2
-1
0
1
2
3
rapidity of top quark

Fig. 4